Modeling and Simulation of a Single Phase Grid Connected Photovoltaic System

AMAL A. HASSAN[1], FATEN H. FAHMY[1], ABD EL-SHAFY A. NAFEH[1], MOHAMED A. EL-SAYED[2]

[1]Photovoltaic Cells Department,
Electronics Research Institute,
National Research Center Building, Cairo,
EGYPT.

[2]Centre of Energy Studies,
University of Trinidad and Tobago,
TRINIDAD AND TOBAGO.

Abstract: - This paper gives a complete computer simulation program of a single phase grid connected PV system using Matlab/Simulink and SimPowerSystem tool in order to monitor the performance of each unit of the system during a selected day in the year representing a sunny day and another cloudy day using the hourly data of load demand, solar radiation and temperature at The Kharga Oasis site, as a case study. The system consists of a PV array subsystem as the primary source of energy, the electric grid as an auxiliary source of energy, the battery bank as a stand by source that feeds the electrical load in case of grid failure. This paper also focuses on the operation control of the system. This control is on/off switch control according to modes of operation of the system and there is a control of inverter using PI controller to achieve the maximum power point of the PV array. Finally this paper gives the simulation results of the required system output parameters; PV output power, grid power, load power, battery power, and battery voltage and state of charge.

Key-Words: - Renewable energy, Photovoltaic systems, Electric grid, Modeling, Control, Simulation.

1 Introduction

The configuration of a single phase grid connected PV system is illustrated in Fig. 1. It consists of solar PV array, input capacitor, single phase inverter, low pass output filter and grid voltage source. The solar PV modules are connected in a series-parallel configuration to match the required solar voltage and power rating. The direct current (DC) link capacitor maintains the solar PV array voltage at a certain level for the voltage source inverter.

The single phase inverter with the output filter converts the DC input voltage into AC sinusoidal voltage by means of appropriate switch signals and then the filter output pass through an isolation step up transformer to setup the filter output voltage to 220 V_{RMS} required by the electric utility grid and load. The system also consists of a battery bank for supplying the electrical loads of the clinic in case of electric grid failure.

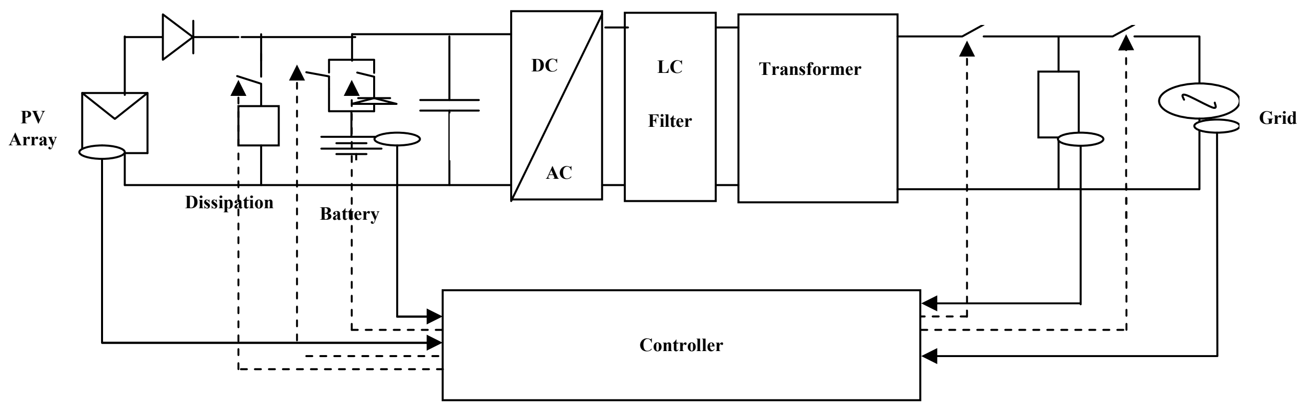

Fig. 1 Block diagram of a single phase grid connected PV system.

2 PV Array Mathematical Model and Implementation

The modules in a PV system are typically connected in arrays in series and parallel configurations. Electrical modeling of suggested PV array system is represented in the following equations [1]:

$$V_{PV} = \left(\frac{B \times K \times T \times N_S}{q} \right) \times ln \left(\frac{N_P (I_L + I_{os}) - I_{PV}}{N_P \times I_{os}} \right) \tag{1}$$

$$I_{os} = I_{or} \left[\frac{T}{T_r} \right]^3 exp \left(\frac{qE_{GO}}{BK} \left(\frac{1}{T_r} - \frac{1}{T} \right) \right) \tag{2}$$

$$I_L = \left[I_{sc} + K_1 (T_c - 28) \right] \times \frac{H}{1000} \tag{3}$$

$$T_c = T_{air} + 0.2 \times H\% \tag{4}$$

Where, V_{PV} is the PV array output voltage (V), I_{PV} is the PV array output current (A), N_S is the number of cells connected in series, N_P is the number of cells connected in parallel, I_L is the light generated current (A), I_{or} is the reverse saturation current (19.97×10^{-6}), B is the ideality factors (1.92), K is the Boltzmann's constant (1.38×10^{-23} joule/ºK), q is the electronic charge (1.602×10^{-19} coulomb), T_r is the reference temperature (301ºK), I_{os} is the cell reverse saturation current (A), T_c is the cell temperature (ºC), T is the cell temperature (ºK), K_1 is the short-circuit current temperature coefficient (0.0017 A / ºC), H is the cell illumination (W/m^2), I_{SC} is the module short-circuit current at 28 ºC and 1000 W/m^2 (4.8 A), E_{GO} is the band gap for silicon (1.11 e.v).

Fig. 2 presents the simulink block diagram of the PV array subsystem, the PV array current is used as an input feedback from the electrical circuit and the output is the PV array voltage and the PV array power.

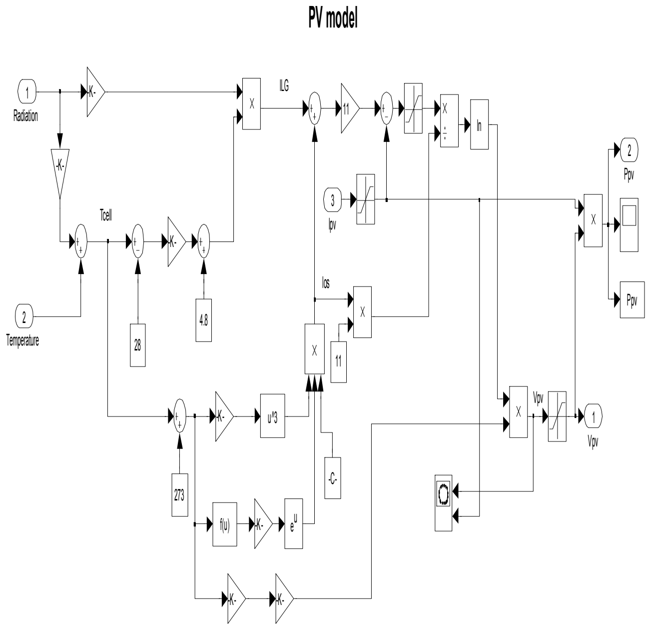

Fig. 2 Block diagram of PV array subsystem.

3 Battery Mathematical Model and Implementation

The battery model is based on a lead acid battery model. Lead acid battery cells consist of two plates, positive and negative, immersed in a dilute sulfuric acid solution. The positive plate, or anode, is made of lead dioxide (PbO_2) and the negative plate, or cathode, is made of lead (Pb). The battery model has two modes of operation: charge and discharge. The battery is in charge mode when the battery input current is positive while the discharge mode is in case of the current is negative. The terminal voltage (V_b) of the battery is given by [2]:

$$V_b = V_1 + I_b \times R_1 \tag{5}$$

Where, V_1, I_b and R_1 are the battery open circuit voltage (V), battery current (A) and the internal resistance of the battery (Ω) respectively. V_1 and R_1 are governed by a set of equations depending on which mode of operation the battery is in.

3.1 Charge Mode

The battery voltage and state of charge (SOC) during charging mode can be described using the following equation [2]:

$$V_1 = V_{ch} = \left[2 + 0.148 \times SOC(t) \right] \times ns \tag{6}$$

$$R_1 = R_{ch} = \frac{0.758 + \frac{0.1309}{\left[1.06 - SOC(t)\right]} \times ns}{Q_m} \tag{7}$$

3.2 Discharge Mode

During discharging, the battery voltage – SOC relationship is given by [2]:

$$V_1 = V_{dch} = \left[1.926 + 0.124 \times SOC(t)\right] \times ns \tag{8}$$

$$R_1 = R_{dch} = \frac{0.19 + \frac{0.1037}{\left[SOC(t) - 0.14\right]} \times ns}{Q_m} \tag{9}$$

Where, $SOC(t)$ is the current state of charge, ns is the number of 2V battery cells in series and Q_m is the maximum battery capacity (Wh). The $SOC(t)$ is the ratio between the present capacity and the nominal capacity and can be estimated using the following equation [2]:

$$SOC(t) = SOC(t-1) + \int_{t-1}^{t} \left(\frac{K_b \times V1 \times I_b}{Q_m} - SOC(t-1) \times D \right) dt \tag{10}$$

Where, K_b is the battery charge/discharge efficiency and D is the battery self discharge rate (h^{-1}). The $SOC(t)$ can be found by knowing the previous condition. Since SOC(0) = SOC1 = initial state of charge, SOC(1) can be found.
Fig. 3 shows the lead acid battery bank subsystem implementation in the Simulink toolbox. There is only one input to this subsystem (I_b) and the outputs of the system are battery voltage (V_b), battery power (P_b) and battery state of charge (SOC).

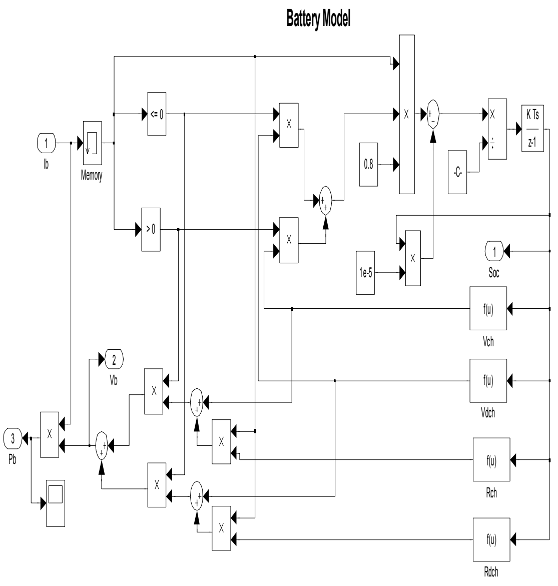

Fig. 3 Block diagram of battery subsystem.

4 Inverter Model

Single phase inverters are used to convert the DC output voltage of the PV array into AC voltage required for an AC load or to be connected to the electric utility grid. The single phase full bridge voltage source inverter circuit configuration is shown in Fig. 4. It is composed of a DC voltage source (PV array), an input decoupling capacitor C and four power switching blocks. C is used to filter the noise on the DC bus. After the inverter an LC harmonic filter is used to eliminate the high frequencies in the output inverter voltage. Each block of the switching blocks consists of a semiconductor switch (IGBT) and an anti-parallel diode. AC output voltage is created by switching the full bridge in an appropriate sequence [3-5].
To create proper gating signals for switches, pulse width modulation (PWM) is used. A high-frequency signal is compared with a specific sinusoidal signal with specific frequency. A PWM inverter output with filtering generally meets the total harmonic distortion (THD) requirements for different applications. The two main advantages of PWM are the control of the output voltage amplitude and fundamental frequency as well as decreasing the filter requirements for minimizing the harmonics. The reference waveform is called the modulation or control signal and it is compared to a carrier signal. Carrier signal is usually a triangular signal which controls the switching frequency while the reference signal controls the output voltage amplitude and its fundamental frequency [3, 4].

5 Output Filter Model and Design

Output filter of the full bridge is filtered using a low pass filter to create a clean output sinusoidal voltage. The LC low pass filter is a second order filter which eliminates all high order harmonics from PWM waveform so that the inverter output is 50 Hz, low distortion, pure sinusoidal output voltage wave [6]. The cut off frequency of the low pass filter (f_c) is selected such that the output total harmonic distortion (THD) is less than 5% [5]. The value of f_c is kept below 1/25th of the inverter switching frequency. The filter inductor value (L_f) is calculated such that the voltage drop across the inductor is less than 3% of the inverter output voltage (V_f) as given in (12) [6, 7]:

$$I_{load\ max} \times 2\pi f L_f < 0.03 V_f \tag{11}$$

Where, $I_{loadmax}$ is the maximum RMS load current, V_f is the RMS value of inverter output voltage and f is the output frequency (50 Hz). The filter capacitance value (C_f) is then calculated from the resonance relation:

$$C_f = \frac{1}{(2\pi f_c)^2 L_f} \tag{12}$$

6 System Control

All power systems must have a control strategy that describes the interactions between its components. There are two main modes of operation for the proposed grid connected PV system; grid connected PV system without battery, while in case of grid failure, the system operates as stand alone PV system with battery storage. The control is achieved using ON/OFF switch logic controller for the system according to these modes of operation. This controller is based on sensing of the grid status, PV array output power, load power and state of charge (SOC) of the battery and compare them to each other or to a reference value and then send a control signal to the system switches to open or close according to the mode of operation. Table 1 summarizes the modes of operation of the proposed system. P_L, P_{PV}, P_G, P_B, and P_{Diss} are the load power, PV array output power, Grid power, Battery power and dissipated power respectively.

Table 1
Modes of Operation of the Proposed Grid Connected PV System

Mode of operation	Grid connected PV system	Stand alone PV system
$P_{PV} = 0$	$P_L = P_G$	$P_L = P_B$
$P_{PV} <= P_L$	$P_L = P_{PV} + P_G$	$P_L = P_{PV} + P_B$
$P_{PV} > P_L$, $SOC >= SOC_{max}$	$P_G = P_{PV} - P_L$	$P_B = 0$, $P_{Diss} = P_{PV} - P_L$
$P_{PV} > P_L$, $SOC < SOC_{max}$	$P_G = 0$, $P_B = P_{PV} - P_L$	$P_B = P_{PV} - P_L$

7 Maximum Power Point Tracking (MPPT)

Tracking the maximum power point (MPPT) of a PV array is usually an essential part of a PV system. A linear current control is used based on the fact that a linear relationship exists between I_{MPP} and the level of solar radiation. The current I_{MPP} is thus found by sensing the solar radiation level using look-up table method [8-10]. In this case, the measured values of PV current are compared to reference values, which correspond to the operation in the maximum point under standard climatological conditions. This will be implemented using a simple current feedback loop with a Proportional Integral (PI) controller which used such that PV array current follows I_{MPP} .The control signal used as a suitable modulation technique like pulse width modulation (PWM). The modulation index of the PWM inverter will be used to control the output power so as to operate at MPP. The block diagram of the control scheme used is shown in Fig. 4 [8-10].

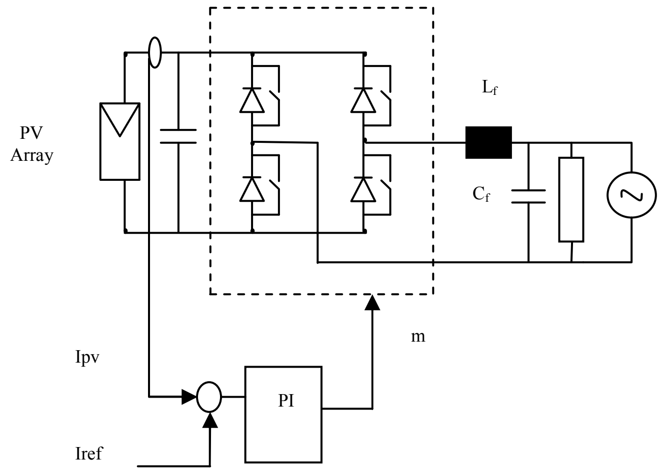

Fig. 4 Control of Full bridge single phase voltage source PWM inverter.

Fig. 5 shows the simulink block diagram for the simulated PV solar array and battery interfaced with the utility grid through pulse width modulation (PWM) driven voltage source inverter and its control. The DC/AC inverter is simulated as a universal bridge from Matlab library, this bridge consists of four switches (IGBT's) with anti-parallel diodes as discussed above. The electric utility grid represented by a single phase AC voltage source.

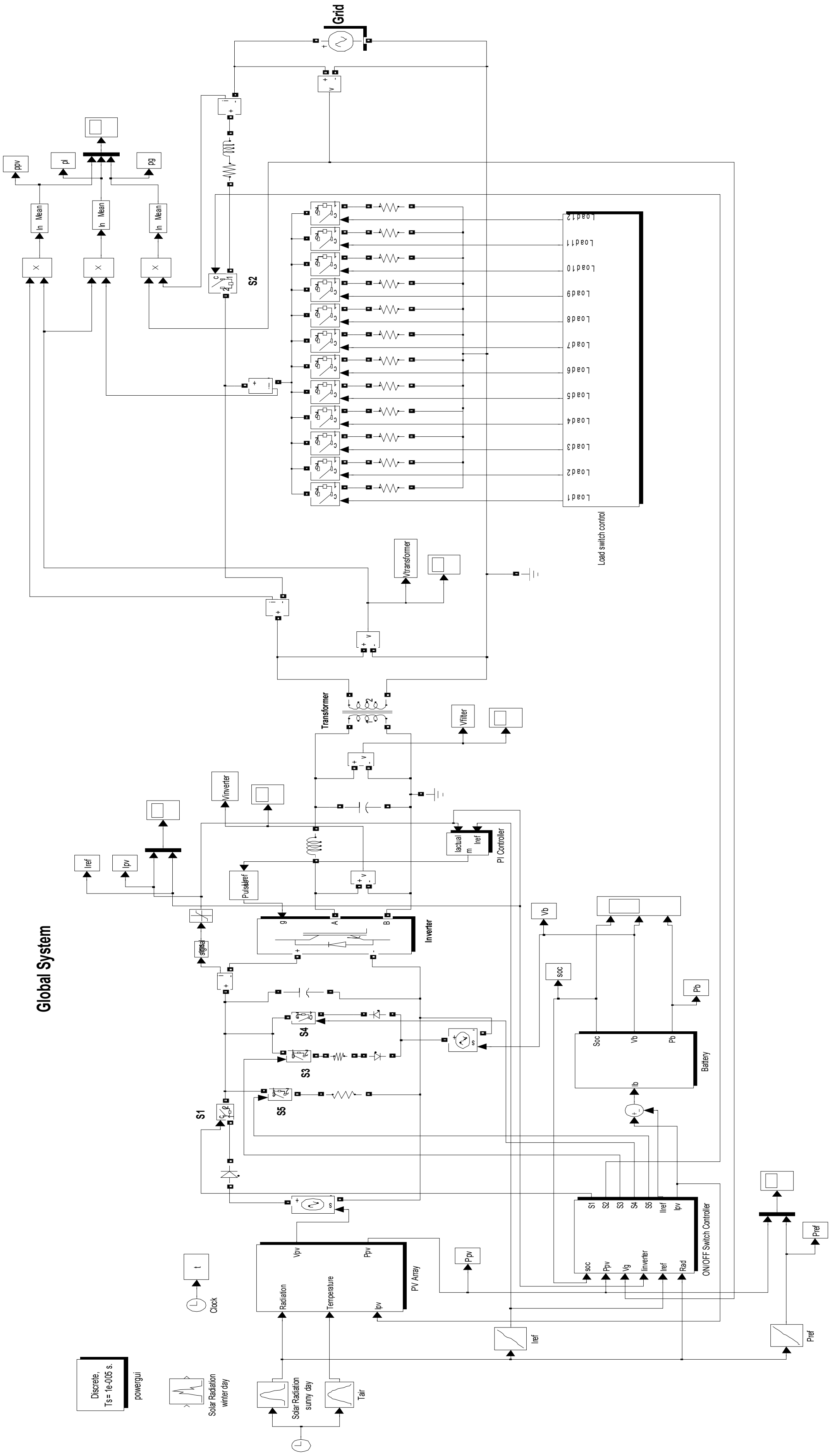

Fig. 5 Block diagram of the system as implemented in Matlab Simulink.

8 Results and Discussion

8.1 PV Subsystem Results

Fig. 6 represents the controlled PV array output current against the reference maximum current. This is performed using different constant values of solar radiation. The maximum value of PV array current changes according to the solar radiation based on a linear relationship that exists between solar radiation and PV array output current. It is also clear from this figure that the system controller tracks the maximum current and so the PV array operates at maximum power point. For studying system behaviour under different circumstances over a complete day, variable radiation profiles are taken representing sunny day and cloudy day. Fig. 7 illustrates the PV output power versus maximum reference power for a sunny day, it is clear that the system tracks the maximum power point. The reference power values have been taken under standard climatological conditions. It also observed from curves that the shape of power curves is the same that of solar radiation curve as shown in Fig 8 which illustrates the incident solar radiation over the Kharga Oasis in W/m^2 starting from 0 at 5 AM and increasing as the sun rises until reaching a maximum value at 12 PM and decreasing again until sunset at 7 PM.

Simulation also was done using a radiation values for a cloudy day. Fig. 9 illustrates the PV array output power versus maximum power. It is observed from these figures that the solar radiation decreases and increases according to the existence of clouds and so the PV output power decreasing and increasing along the day taking the shape of solar radiation curve represented in Fig. 10. It can also be noted that the PI controller of the inverter tracks the maximum power point as the power curves of the PV output power and reference maximum power under these climatological conditions almost coincides.

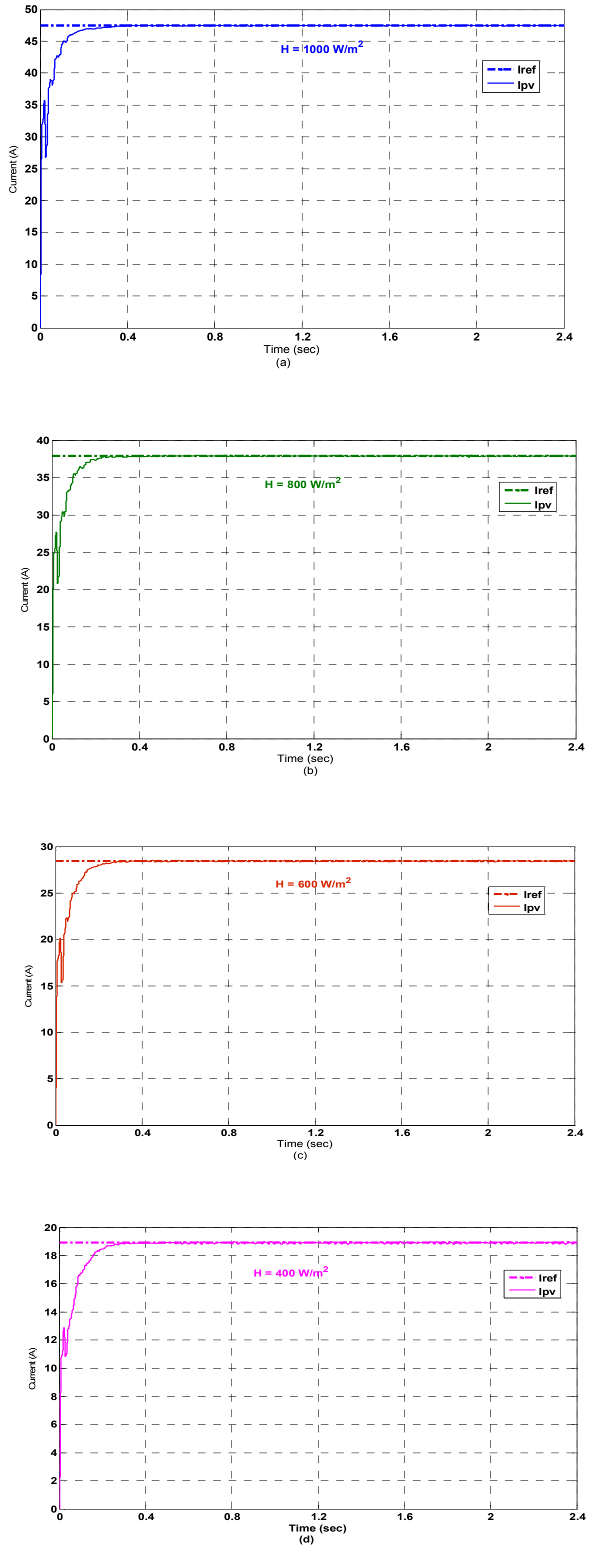

Fig. 6 The simulated PV array output currents for constant radiation values against reference maximum current.

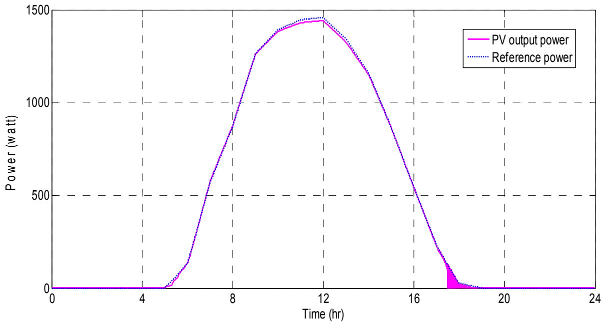

Fig. 7 Maximum PV output power and reference maximum power for a sunny day.

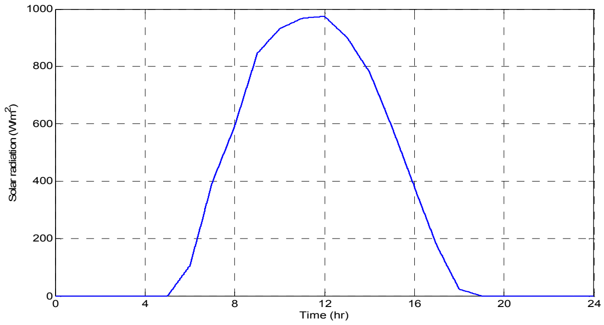

Fig. 8 The incident solar radiation over The Kharga Oasis in W/m^2 for a sunny day.

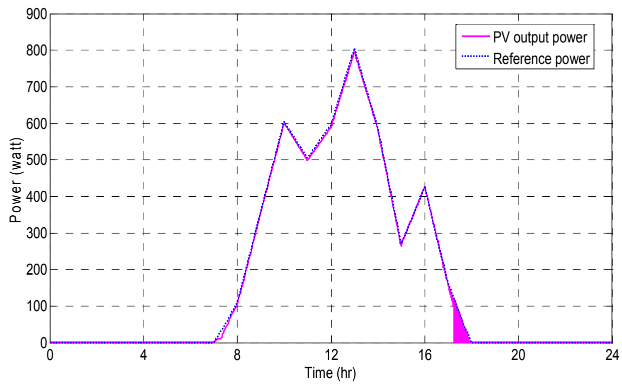

Fig. 9 Maximum PV output power and reference maximum power for a cloudy day.

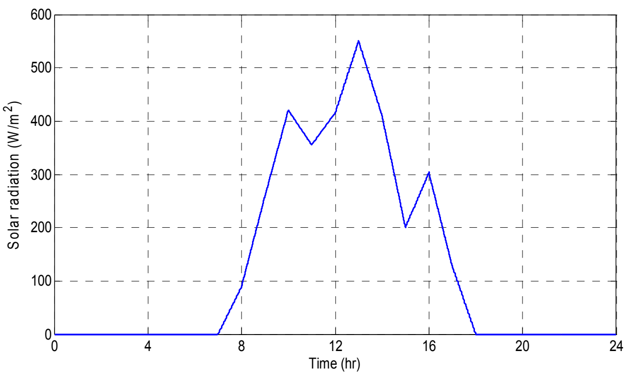

Fig. 10 The incident solar radiation over The Kharga Oasis in W/m^2 for a cloudy day.

8.2 Grid-Connected Mode Results

Fig. 11 shows the average power curves of the grid connected PV system for a sunny day. During night and early morning, the load is fed completely from the utility grid (S1 is off and S2 is on). At sunshine, the PV power becomes greater than 0 and the load is fed firstly from the PV array and the deficit power is supplied from the utility grid (S1 is on and S2 is on) while at peak sun hours from 7 AM to 8 AM and from 9 AM to 4 PM, the PV output power is greater than the load power and so the excess power is delivered to the electric grid. The average power curves of grid connected PV system for a cloudy day are illustrated in Fig. 12, the PV output power is low and the grid supply the deficit energy until 12 PM, so the power sold to the electric utility grid is lower than the power sold during sunny days.

The value of energy sold to the electric utility grid is 2.941 kWh/day for a sunny day and 0.42125 kWh/day for a cloudy day. Where, the energy purchased from the electric utility grid during cloudy days (10.74 kWh/day) is higher than the energy that purchased during sunny days (8.31 kWh/day) regarding that the load power consumption during summer is higher.

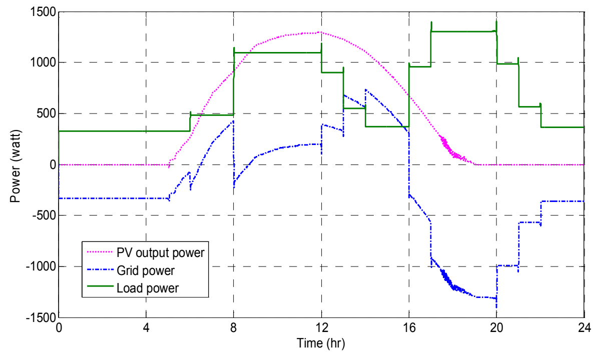

Fig. 11 Simulated generated power of PV, electric utility grid and load consumption for a sunny day.

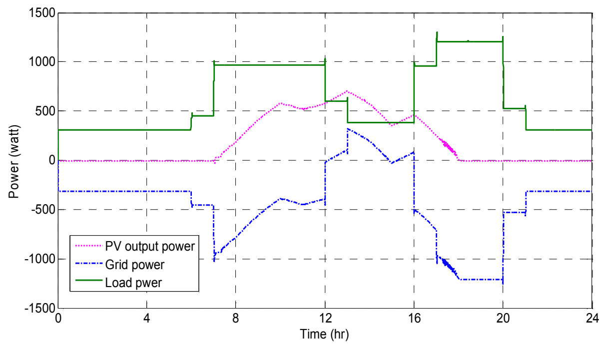

Fig. 12 Simulated generated power of PV, electric utility grid and load consumption for a cloudy day.

Fig. 13.a shows the current injected by the PV solar array after passing through power conditioning equipments (inverter, filter and transformer) with total harmonic distortion (THD) 0.81 %, the grid line current with THD of 1.08 % and the load current with THD 0.23%. The time interval of that figure is the early morning and sunshine period when the PV array starts to generate electrical power. The load is fed from utility grid, and then when the PV power exists, the load is fed from PV array and the deficit energy will be supplied from the utility grid. In the other hand, Fig. 13.b represents the current injected by the PV solar array, the grid line current and the load current during peak sun hour's period. It is observed that PV output current is higher than load current and so the surplus energy is being injected to the utility grid. During night, the PV output current is zero as shown in Fig. 13.c. It is also so clear that the load current and grid line current coincide which means that the load is fed completely from utility grid.

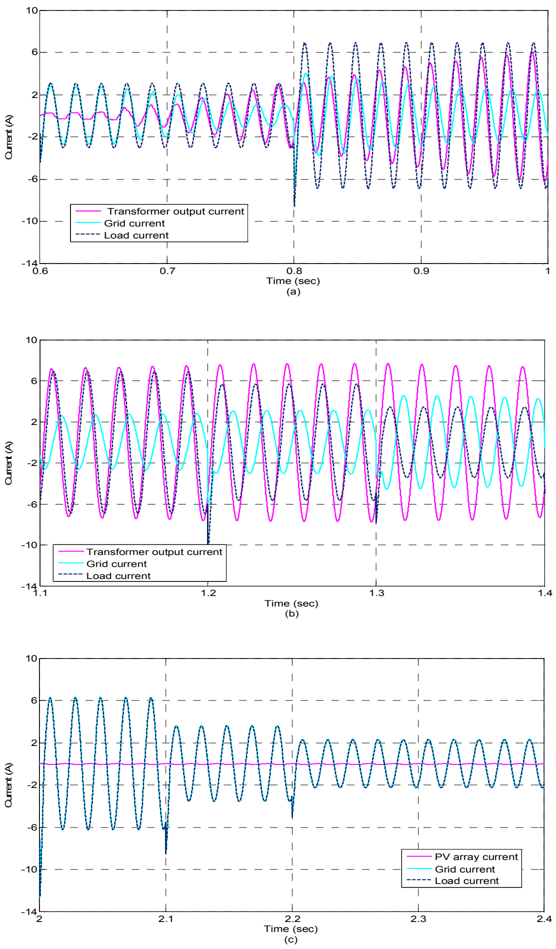

Fig. 13 Simulated transformer output current, grid current and load current.

8.3 Stand-Alone Mode Results

The stand alone mode contains the operation of the battery bank subsystem. The battery bank was designed to operate in parallel with the PV subsystem and feed the electrical loads of the clinic for a complete day in case of grid failure. Fig. 14 presents the battery power for a sunny day. As illustrated in the figure, in case of grid failure and during night and early morning hours, all load power demand is being discharged from the battery (S1 off, S2 off, S3 on and S4 off). Then, the PV output power increases but the load power increases and the power discharged from battery is the difference between the output PV power and load power (S1 on, S2 off, S3 on and S4 off). The discharged battery power then decreases as the PV power increases and when the PV array output power exceeds the load demand, this power is being delivered to the battery bank to be charged (S1 on, S2 off, S3 off and S4 on). In charging mode, the battery power is positive value from 7 AM up to 4 PM. After peak sun hours, the PV output power decreases and the deficit power is being discharged again from the battery bank.

Fig. 15 shows the battery power during a cloudy day, due to low generation the battery is heavily discharged to supply the deficit energy during day hours and completely fed the electrical loads during night. There is excess power only to the battery to be charged from 1 PM to 2 PM.

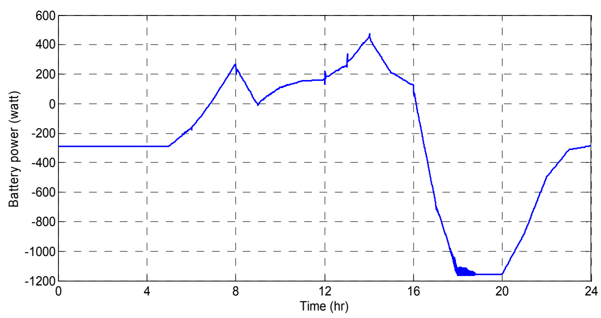

Fig. 14 Simulated battery power during a sunny day.

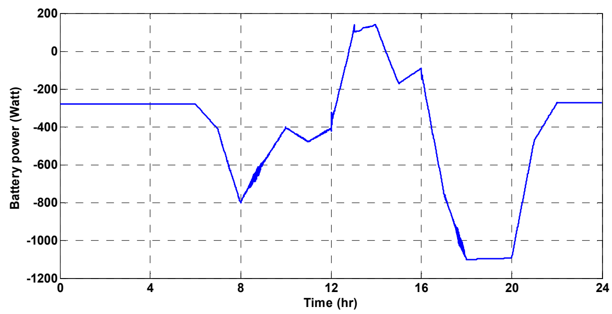

Fig. 15 Simulated battery power during a cloudy day.

The state of charge (SOC) of the battery is presented in Fig. 16 which gives an indication of the battery capacity level. It starts from 100% and then decreases as the battery at the discharging mode reaching a value of 92.5%. During charging, the SOC increases until 100% and decreasing again at discharging until reaching 75% at the end of the day. It is observed from SOC curve for a cloudy day as shown in Fig. 17 that the battery discharged to 57.7% at the end of the day and the excess power during day hours cannot charge the battery to its full capacity as sunny days due to low radiation levels in cloudy days and intermittent PV output power generation.

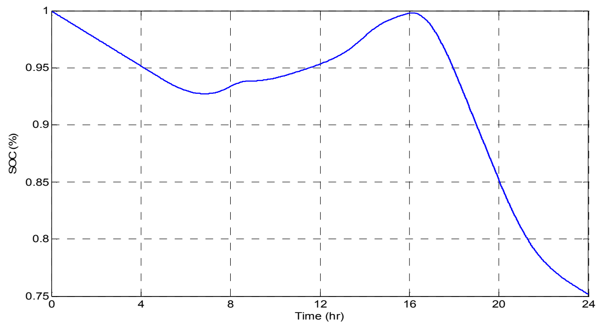

Fig. 16 Simulated SOC during a sunny day.

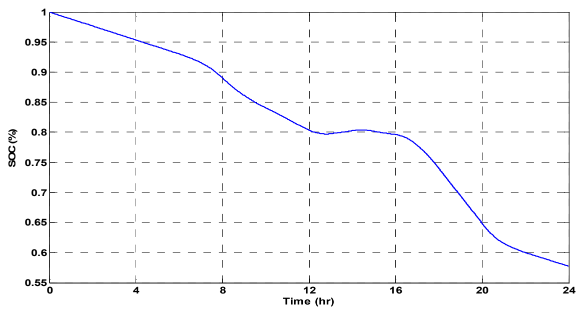

Fig. 17 Simulated SOC during a cloudy day.

8.4 Inverter results

The inverter works with a pulse width modulation technique. The IGBT switches are driven by a pulse generator controlled via PI controller which gives it the value of modulation index (m). Fig. 18 introduces the output pulse width modulation voltage of the inverter, which is represented by a square modulated AC wave. But it is shown that this signal contains high frequency switching harmonics, which can be eliminated by using low pass filter. The total harmonic distortion (THD) is very high reaching a value of about 67.38%.

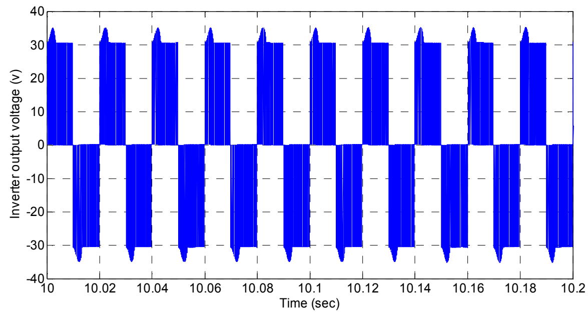

Fig. 18 Simulated PWM inverter output voltage.

8.5 Filter results

The cut off frequency of the filter is much higher than the signal fundamental frequency. The output voltage of filter is shown in Fig. 19 as pure sine wave with almost no harmonic contents and. The THD is 1.01% (below the world standard 3%) representing a very good signal to be delivered to the electrical grid and load.

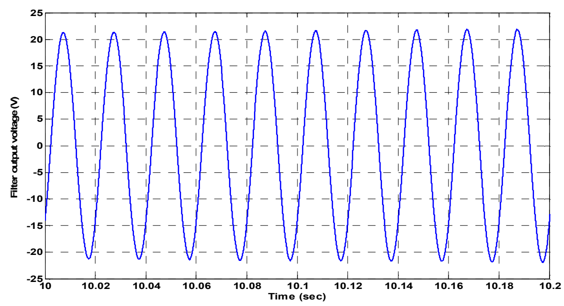

Fig. 19 The simulated filtered output voltage of the inverter.

8.6 Transformer Results

Transformer output voltage is shown in Fig. 20, it is clear that the transformer output voltage is almost pure sine wave of 220 VRMS value and 50 Hz fundamental frequency representing a very good signal consistent with the utility grid load requirements.

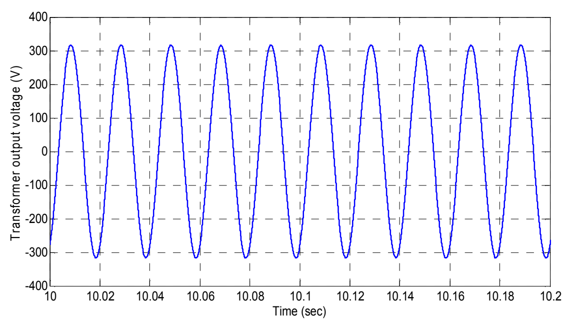

Fig. 20 Simulated transformer output voltage.

9 Conclusion

In this paper the mathematical model of all system components was introduced in order to investigate the dynamic behavior of each subsystem. Also the proposed control technique of the system was presented. This includes ON/OFF switch control of the system according to the modes of operation and inverter control using PI controller to track the maximum power point. The proposed system components models are implemented in Matlab/Simulink environment and interfaced with SimPowerSystem toolbox. The dynamic behavior of each subsystem is investigated showing the interaction between different components of grid connected PV system. The system gives a very good behavior for grid connected PV system mode and stand alone mode. The electrical loads of the clinic are completely supplied with electrical energy. The maximum power point is achieved. In case of stand alone mode and with the worst mode of operation (grid failure and cloudy day), the system gives good performance and the electrical loads are also completely supplied with electrical energy during the day. In that mode, the battery discharged until 57.7% above the discharging limit (30%) which means that there is a reserve capacity in the battery bank. The power conditioning units are well designed as the total harmonic distortion (THD) in the output voltage of the filter is 1.01% (below the world standard 3%) representing a very good signal to be delivered to the electrical grid and load. the current injected by the PV solar array after passing through power conditioning equipments (inverter, filter and transformer) has a THD of 0.81 %, the grid line current has a THD of 1.08% and the load current has a THD 0.23%.

References:

[1] Eftichios Koutroulis, Kostas Kalaitzaiis and Nicholas C. Voulgaris, Development of a microcontroller-based, photovoltaic maximum power point tracking control system, *IEEE Transactions on Power Electronics*, Vol. 16, No.1, Jan., 2001, pp. 46-54.

[2] Castaner Luis and Santiago Silvestre, *Modeling Photovoltaic systems using PSpice*, John Wiley and Sons Ltd, 2002.

[3] Arman Roshan, A dq rotating frame controller for single phase full-bridge inverters used in small distributed generation systems, *M.Sc. thesis*, Faculty of the Virginia Polytechnic Institute and State University, Jun., 2006.

[4] Dehbonei H., Borle L. and Nayar C.V., A review and a proposal for optimal harmonic mitigation in single-phase pulse width modulation, *Proceedings of 4th IEEE International Conference on Power Electronics and Drive Systems*, 2001, Vol. 1, Oct., 2001, pp. 408 – 414.

[5] Hossein Madadi Kojabadi, Bin Yu, Idris A. Gadoura, Liuchen Chang and Mohsen Ghribi, A Novel DSP-Based Current-Controlled PWM Strategy for Single Phase Grid Connected Inverters, *IEEE Transactions on Power Electronics*, Vol. 21, No. 4, Jul., 2006, pp. 98

[6] Khaled H. Ahmed, Stephen J. Finney and Barry W. Williams, Passive Filter Design for Three-Phase Inverter Interfacing in Distributed Generation, *Journal of Electrical Power Quality and Utilisation*, Vol. XIII, No. 2, 2007, pp. 49-58.

[7] E.Koutroulis, J.Chatzakis, K.Kalaitzakis and N.C.Voulgaris, A bidirectional, sinusoidal, high-frequency inverter Design, *IEE Proc.-Electr. Power Appl.*, Vol. 148, No. 4, Jul., 2001, pp. 315-321.

[8] V. Salas, E. Olı´as, A. Barrado and A. La´zaro, Review of the maximum power point tracking algorithms for stand-alone photovoltaic systems, *Solar Energy Materials & Solar Cells*, Vol. 90, 2006, pp. 1555–1578.

[9] S. Yuvarajan, Dachuan Yu and Shanguang Xub, A novel power converter for photovoltaic applications, *Journal of Power Sources*, Vol. 135, 2004, pp. 327–331.

[10] Trishan Esram, and Patrick L. Chapman, Comparison of Photovoltaic Array Maximum Power Point Tracking Techniques, *IEEE Transactions on Energy Conversion*, Vol. 22, No. 2, Jun., 2007, pp. 439-449.